This article has been accepted for publication in a future issue of this journal, but has not been fully edited. Content may change prior to final publication. Citation information: DOI 10.1109/TSTE.2018.2878924, IEEE Transactions on Sustainable Energy

A Parameter Estimation based MPPT Method for a PV System using Lyapunov Control Scheme

Amir Hussain, Man Mohan Garg, *Member, IEEE*, Meher Preetam Korukonda, Shamim Hasan, and Laxmidhar Behera, *Senior Member, IEEE*

***Abstract*—There are two types of external variations which change the operating point of a photovoltaic (PV) system: one is environmental change caused by variation in temperature and/or irradiance and the other is load change. The variation in environmental condition changes the PV array characteristic itself whereas the load variation changes the operating point within the same curve. Each type of change can be uniquely identified using history of PV voltage and current measurements. Using the above fact, this paper proposes a fast maximum power point tracking (MPPT) technique for PV array coupled with boost converter. The proposed method determines MPP in a single step by finding out temperature and irradiance at which the PV array is operating. Furthermore, based on the measured values of PV voltage and current, inductor current and load voltage are also calculated, eliminating the need for additional sensors. Lyapunov based controller (LBC) is implemented to track inductor current to its desired value and find the desired duty cycle to reach MPP. The proposed method is validated by both simulation and experimental results under varying temperature, irradiance and load condition. A comparison with the existing MPPT method is also presented in order to show the efficacy of the proposed method.**

***Index Term*—DC-DC converters, Incremental Conductance, Lyapunov Function, MPPT, Parameter Estimation,PV cell**

NOMENCLATURE

I_g	Photogenerated current of a single PV cell
i_{pv}	Output current of the PV array
v_{pv}	Output voltage of the PV array
I_s	Reverse saturation current of diode
r_s	Series resistance of a single cell
r_{sh}	Parallel resistance of a single cell
n_s	Numbers of series cells in PV array
n_p	Numbers of parallel cells in PV array
R_s	Series resistance of PV array
R_{sh}	Parallel resistance of PV array
p	Diode ideality constant
T	Actual cell temperature
T_r	Reference cell temperature (298 K)
λ	Actual irradiance
λ_r	Reference irradiance (1000 W/m^2)
k_i	Short-circuit current temperature coefficient.
I_{sc}	Short-circuit current at STC (298 K & 1000 W/m^2
q	Electron charge (1.6×10^{-19} C)
K	Boltzmann constant ($1.38 \times 10^{-23} J/K$)
E_{gp}	Energy bandgap (1.1 eV)

I. INTRODUCTION

In the present day scenario, solar photovoltaic energy is considered as a viable alternative to the conventional energy sources such as thermal, gas, nuclear, etc. Therefore, research is being carried out on various issues related to electric power generation for different applications using photovoltaic (PV) energy sources [1]- [4]. PV energy system has several advantages such as pollution-free, abundant availability, less maintenance and near zero carbon emission. However, the non linear current voltage (I-V) characteristic of PV arrays makes it necessary to operate at MPP in order to extract maximum power from it. There are many MPPT algorithms reported in the literature [5]- [7]. Efficient MPPT algorithms should impel PV systems to harvest maximum power available irrespective of the change in atmospheric condition or load. The popular MPPT algorithms are mainly based on different techniques like perturb and observe (P&O) [8] [9], incremental conductance (INC) [10] [11], hill climbing, fractional open-circuit voltage [12], fractional short-circuit current [13], ripple correlation control [14], fuzzy logic control [15], [16], particle swarm optimization [17], [18], artificial neural network [19], genetic algorithm [20]. These algorithms differ from one another based on their ease of implementation, tracking speed, number of sensors used, tracking efficiency, cost, etc. The P&O MPPT technique is quite straight forward in computation and can easily be implemented using any low-cost microcontroller. However, in steady-state, the output power oscillates around the MPP resulting in inefficient extraction of available power [9]. These power oscillations can be minimized by reducing the voltage step size, but it takes more time to reach the MPP. Moreover, during rapid change in environmental conditions, there is a possibility that the operating point of PV system may deviate from MPP [21].

In [22], a variable step INC method (VSINC) was proposed where the voltage step size is adaptively varied based on the rate of change of power with voltage. Even then, as the operating point reaches MPP, the step size reduces to a smaller value which requires more time to converge. However, in this technique also, settling time to reach MPP is high because the voltage step size is reduced to a smaller value as the operating point reached near MPP. Further, a fast converging MPPT (FC-MPPT) method was proposed in [23] which quickly shifts the operating point near to

This article has been accepted for publication in a future issue of this journal, but has not been fully edited. Content may change prior to final publication. Citation information: DOI 10.1109/TSTE.2018.2878924, IEEE Transactions on Sustainable Energy

MPP region using geometric techniques and then applies incremental conductance to reach the actual MPP. However, in case of fast varying environmental and load conditions, this method does not perform well because the obtained approximate operating points tend to be quite far from MPP region as there is no information of the system model being used. The MPPT methods discussed so far gradually arrive at MPP by varying the reference voltage/current values based on certain search criteria. They search for MPP in each step without actually possessing the information about complete characteristics of PV system. Alternatively, many model based MPPT techniques have been proposed in literature [24]- [31]. These techniques capture the complete range of I-V relationship using different models and directly find the MPP using computational means. The PV system is then directly controlled to operate at MPP. Various model estimation techniques using artificial neural networks (ANN) [24] and neuro-fuzzy models [25] were proposed for this purpose. While these techniques find the MPPs accurately, they often suffer from heavy computational burden. Moreover, if there are unprecedented changes in environmental and physical conditions, these models need to be retrained to accurately reflect the changes. On the other hand, physical model estimation techniques using curve-fitting methods have also shown much presence in the recent literature. These techniques solve the different electrical models of the solar cell such as single-diode model [26], double diode-model [27] under controlled conditions and extrapolate them for other working conditions and find the MPP using numerical techniques. Many of these resort to [28], analytical five point method [29] or heuristic techniques like PSO [30] to arrive at the accurate characteristics of the solar cell. An analytical expression was also developed for the direct determination of MPP references using Lambert W function [31]. However, in these model estimation based MPPT methods, additional hardware is required for measuring temperature and irradiance which adds to cost of the overall system.

To eliminate the need of temperature and irradiation sensors, many methods has been developed to estimate the temperature and irradiance and improve detection of the MPP. For instance, [32] proposed a combined model based and heuristic MPPT (CMH-MPPT) which works similar to FC-MPPT method by forcing the operating point to a near MPP zone. However, its performance is superior to that of FC-MPPT during rapid change in environmental conditions due to the additional model based temperature estimation feature included. The limitation of this method is that it cannot reach MPP in a single step. On the contrary, [33] proposed a single-step formula for finding MPP using simplified polynomial analytical model which estimates its parameters in real time without using additional environmental sensors. However, its single-step formula necessitates placement of an additional voltage sensor at the output. It is also observed that in most of these works, the non-idealities of PV models have been neglected for simplicity. To the best of the authors' knowledge, there is no work in the literature to find MPP for fast varying environmental and load conditions in a single step using only voltage and current sensors while considering PV array non-idealities.

In this paper, an algorithm is proposed to for maximum power point tracking in a single step under fast varying environmental and load conditions. First, the ambient irradiation and temperature values are estimated using Newton-Raphson (NR) method. Then, the reference PV voltage and current for the corresponding MPP is calculated. To improve the transient performance during rapid change in environmental conditions or load variations, a Lyapunov based current control technique is also developed. Furthermore, a technique is also developed to calculate the inductor current and output voltage to obviate the necessity of additional sensors. The proposed Lyapunov based current control design is independent of load resistance. The main contributions of the paper are summarized as follows:

1) An online technique for estimation of temperature and irradiation considering non-idealities in PV model.
2) A Lyapunov based current control (LBC) scheme using estimated values of inductor current and load voltage.

II. Mathematical Modeling of PV Array System

The basic PV system configuration and its mathematical description is presented in the following subsections:

A. PV characteristic

The electrical characteristics of a PV cell are usually described by the single-diode model with acceptable accuracy [34]. The equivalent circuit of a single PV cell using single-diode model is shown in Fig.1(a). In practice, PV cells are combined in series and parallel to form a large PV array. The equivalent circuit of a PV array consisting of n_s series and n_p parallel PV cells is shown in Fig.1(b). The current-voltage relationship of the PV array is given by [35]

$$i_{pv} = n_p I_g - n_p I_s \left(e^{\frac{q(v_{pv} + i_{pv} R_s)}{n_s p K T}} - 1 \right) - \frac{v_{pv} + i_{pv} R_s}{R_{sh}} \quad (1)$$

The photo-generated current I_g is a function of temperature and irradiance and is given as

$$I_g = (I_{sc} + k_I (T - Tr))\lambda / \lambda_r \quad (2)$$

The reverse saturation current I_s is formulated as

$$I_s = I_r \left(\frac{T}{T_r} \right)^3 e^{qE_{gp}\left(\frac{1}{T_r} - \frac{1}{T}\right)/pK} \quad (3)$$

As discussed earlier, the variations in irradiance and temperature affect the power output of the solar PV array. Similarly, series and shunt resistances also affect the output power. These effects have been portrayed in the P-V characteristics as shown in Fig.2. It may be observed that although R_s and R_{sh} have least effect in open circuit and short circuit region, they greatly influence the P-V characteristic in MPP region. Therefore, it is important to take them into consideration while estimating actual T and λ using I-V curve. The variation of R_s and R_{sh} with temperature and

This article has been accepted for publication in a future issue of this journal, but has not been fully edited. Content may change prior to final publication. Citation information: DOI 10.1109/TSTE.2018.2878924, IEEE Transactions on Sustainable Energy

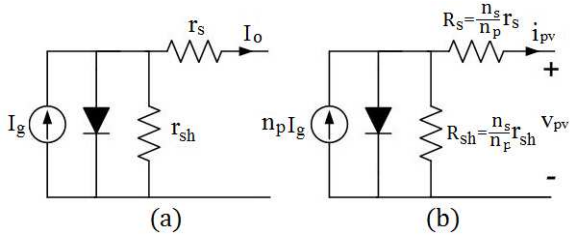

Fig. 1. Equivalent circuit of (a) Single PV cell (b) Complete PV array

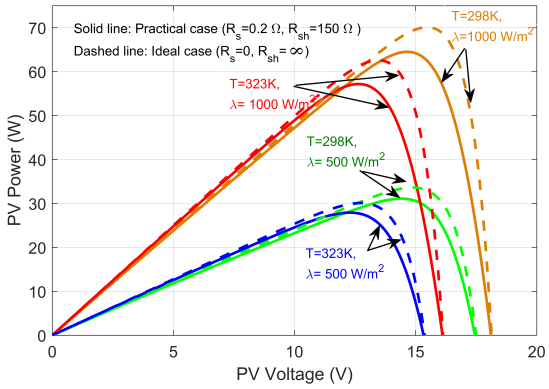

Fig. 2. Effect of series and shunt resistance of P-V curve for different temperature and irradiance.

irradiance has negligible effect on characteristics of PV array [36], [37]. Therefore, they are assumed constant throughout the paper.

B. Power Converter

Fig. 3 shows a PV array connected to a dc-dc boost converter. Power output from PV module is controlled by varying the duty ratio of boost converter so as to operate at MPP. The PV system along with boost converter is a third order non-linear system. Taking inductor current i_L, PV voltage v_{pv} and load voltage v_o as system states, the time averaged state space model of boost converter [38] is described as follows,

$$\dot{i}_L = \frac{1}{L}\left(v_{pv} - r i_L - V_D - v_o\right) + \frac{1}{L}(V_D + v_o)u \quad (4)$$

$$\dot{v}_{pv} = \frac{1}{C_a}\left(i_{pv} - i_L\right) \quad (5)$$

$$\dot{v}_o = \frac{1}{C_b}\left(i_L - \frac{v_o}{R_{ld}}\right) - \frac{1}{C_b} i_L u \quad (6)$$

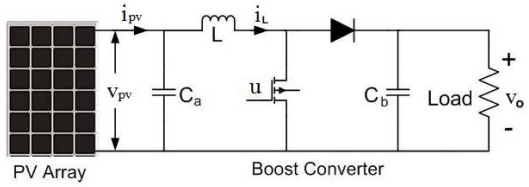

Fig. 3. PV Array in conjunction with dc-dc boost converter.

Here C_a : PV capacitor, C_b : output capacitor, V_D : diode voltage drop, r : resistance of inductor, R_{ld} : load resistance. u is a switching signal which is 1 when switch is on and 0 when switch is off.

III. Temperature and Irradiance Detection

The I-V characteristics of a particular PV array depends on a number of parameters as described in equations (1) to (3). Temperature and irradiance level can be considered as external parameters which change with environmental condition. Other parameters like ideality factor and modeled resistances of PV array are considered as internal parameters which are known and constant. Therefore, variation in I-V characteristic corresponds to the variation in PV array external parameters. These parameters can be calculated by plugging in different sets of sensed PV array voltage and current values in system equation. Since the I-V characteristic follows a non linear relation, NR method is used to find the system parameter as it converges faster than other techniques.

The I-V relation can be written as function of internal and external parameters as

$$i_{pv} = f(\mathbf{x}, T, \lambda, v_{pv})$$

where $\mathbf{x}$ is set of internal parameters of PV array which are considered constant.

Following the prescripts of NR Method, it is assumed that (v_1, i_1) and (v_2, i_2) are two sets of measured value of PV array voltage and current at time t and $t+\delta t$ while operating at temperature T and irradiance λ. δt is the time interval at which temperature and irradiance are updated. Hence, i_{pv_1} and i_{pv_2} at v_{pv_1} and v_{pv_2} can be written as

$$i_{pv_1} = f(\mathbf{x}, T, \lambda, v_{pv_1}) \qquad i_{pv_2} = f(\mathbf{x}, T, \lambda, v_{pv_2})$$

It is also assumed that $i_{pv_{1k}}$ and $i_{pv_{2k}}$ are the calculated currents at voltages $v_{pv}{}_1$ and v_{pv_2} respectively in the k^{th} iteration corresponding to estimated temperature T_k and irradiance λ_k. Therefore,

$$i_{pv_{1k}} = f(\mathbf{x}, T_k, \lambda_k, v_{pv_1}) \qquad i_{pv_{2k}} = f(\mathbf{x}, T_k, \lambda_k, v_{pv_2})$$

Having known the internal parameters and sets of measured values of PV voltage and current, temperature T_{k+1} and irradiance λ_{k+1} in the next iteration is calculated as follows

$$\begin{bmatrix} T_{k+1} \\ \lambda_{k+1} \end{bmatrix} = \begin{bmatrix} T_k \\ \lambda_k \end{bmatrix} + [J]^{-1} \begin{bmatrix} i_{pv_1} - i_{pv_{1k}} \\ i_{pv_2} - i_{pv_{2k}} \end{bmatrix} \quad (7)$$

where

$$[J] = \begin{bmatrix} \frac{\partial i_{pv}}{\partial T}_{(v_{pv_1}, T_k, \lambda_k)} & \frac{\partial i_{pv}}{\partial \lambda}_{(v_{pv_1}, T_k, \lambda_k)} \\ \frac{\partial i_{pv}}{\partial T}_{(v_{pv_2}, T_k, \lambda_k)} & \frac{\partial i_{pv}}{\partial \lambda}_{(v_{pv_2}, T_k, \lambda_k)} \end{bmatrix} \quad (8)$$

$\frac{\partial i_{pv}}{\partial T}$ is found out by differentiating (1) and then upon simplification is written as

This article has been accepted for publication in a future issue of this journal, but has not been fully edited. Content may change prior to final publication. Citation information: DOI 10.1109/TSTE.2018.2878924, IEEE Transactions on Sustainable Energy

TABLE I
DESIRED VALUES OF PV VOLTAGE, CURRENT AND POWER FOR DIFFERENT ENVIRONMENTAL CONDITIONS

Case	Temperature	Irradiance	v_{pv_r}	i_{pv_r}	P_{pv_r}
I	298K	$500W/m^2$	14.4V	2.15A	31.0W
II	298K	$1000W/m^2$	14.6V	4.40A	64.2W
III	323K	$1000W/m^2$	12.7V	4.52A	57.5W
IV	323K	$500W/m^2$	12.3V	2.26A	28.5W

$$\frac{\partial i_{pv}}{\partial T} = n_p \frac{\partial I_g}{\partial T} - n_p \frac{\partial I_s}{\partial T}\left(e^{\frac{q(v_{pv}+i_{pv}R_s)}{pKn_sT}} - 1\right) - n_p I_s \frac{\partial}{\partial T}\left(e^{\frac{q(v_{pv}+i_{pv}R_s)}{pKn_sT}} - 1\right) - \frac{\partial}{\partial T}\frac{(v_{pv}+i_{pv}R_s)}{R_{sh}} \tag{9}$$

Taking the terms of $\frac{\partial i_{pv}}{\partial T}$ together, we get (10) on the top of next page where,

$$\frac{\partial I_s}{\partial T} = \frac{I_r}{T_r^3}\left(3T^2 + \frac{qE_{gp}T}{pK}\right) e^{\frac{qE_{gp}}{pK}\left(\frac{1}{T}-\frac{1}{T_r}\right)} \tag{11}$$

Similarly $\frac{\partial i_{pv}}{\partial \lambda}$ can be written as

$$\frac{\partial i_{pv}}{\partial \lambda} = \frac{n_p\left(I_{sc}+k_I(T-T_r)\right)}{\lambda_r + \frac{\lambda_r n_p I_s q R_s}{pKTn_s}\left(e^{\frac{q(v_{pv}+i_{pv}R_s)}{pKn_sT}}\right)} \tag{12}$$

NR method converges very quickly and it typically takes 4 to 5 iterations to find out the solution of T and λ. The interval δt is also an important parameter which should be carefully chosen. While higher value of δt makes the detection slower in case of change in environmental conditions, smaller value repetitively calculates the same T and λ with high frequency in case of no environmental change. To overcome this situation, in this paper, the new value of T and λ is estimated only when change in PV voltage/current is greater than a minimum value.

IV. CALCULATION OF DESIRED STATES

Desired states of the system are calculated using state space equations once the PV characteristic is known. PV voltage v_{pv_r} and current i_{pv_r} corresponding to MPP are numerically found out using INC method as done in [39]. Calculation of desired value of inductor current and converter output voltage is performed using steady state analysis.

Let i_{L_r}, v_{pv_r}, v_{o_r} be the desired steady-state values of inductor current, PV voltage and converter output voltage respectively and $e_1 = i_L - i_{L_r}$, $e_2 = v_{pv} - v_{pv_r}$, $e_3 = v_o - v_{o_r}$ be be their corresponding errors. In steady state, when the desired values are reached, all the errors and their derivatives become 0.

$$e_1 = e_2 = e_3 = 0, \dot{e}_1 = \dot{e}_2 = \dot{e}_3 = 0 \tag{13}$$

Therefore, in steady state, (4) to (6) become

$$\frac{1}{L}(v_{pv_r} - ri_{L_r} - V_D + u_r V_D - v_{o_r} + u_r v_{o_r}) = 0 \tag{14}$$

$$\frac{1}{C_a}(i_{pv_r} - i_{L_r}) = 0 \tag{15}$$

$$\frac{1}{C_b}\left(i_{L_r}(1-u_r) - \frac{v_{o_r}}{R_{ld}}\right) = 0 \tag{16}$$

Upon simplifying, (14), (15) and (16) we get,

$$i_{L_r} = i_{pv_r} \tag{17}$$

$$v_{o_r} = \frac{-V_D + \sqrt{V_D^2 + 4i_{pv_r}R_{ld}(v_{pv_r} - ri_{pv_r})}}{2} \tag{18}$$

$$u_r = 1 - \frac{v_{pv_r} - i_{pv_r}r}{V_D + v_{o_r}} \tag{19}$$

where u_r is the desired duy cycle.

Equations (17) to (19) show that the desired steady state inductor current is equal to the reference PV current corresponding to MPP. Although desired PV current for MPP and hence desired average inductor is independent of load, the final output voltage is a function of load resistance which makes the desired duty cycle dependent on load. Table I shows desired values of MPP PV voltage, current and power for different temperature and irradiance levels.

V. LYAPUNOV BASED CONTROL(LBC) SCHEME

Lyapunov design has been a primary tool for nonlinear control system design, stability and performance analysis since its introduction. The central idea is to design a feedback control law that renders the derivative of a specified Lyapunov function (LF) negative definite or negative semi-definite [40] . Different choices of Lyapunov functions may result in different control structures and control performance. In the present system, Lyapunov function is formed using error in inductor current as

$$V = \frac{1}{2}e_1^2 \tag{20}$$

Using (4) and (20)

$$\dot{V} = \frac{1}{L}e_1\left(v_{pv} - ri_L - V_D - v_o + uV_D + uv_o\right) \tag{21}$$

choosing

$$u = \frac{V_D + v_o - v_{pv} + ri_L - K_c L e_1}{V_D + v_o} \tag{22}$$

ensures that

$$\dot{V} = -K_c e_1^2 \tag{23}$$

where K_c is chosen strictly positive to make sure (23) becomes less than zero. This ensures that control action keeps the system stable.

Apart from desired inductor current, the control signal in (22) requires value of PV voltage, actual inductor current and output voltage. In this paper, instead of using expensive voltage and current sensors for sensing output voltage and inductor current, these variables are calculated using the

This article has been accepted for publication in a future issue of this journal, but has not been fully edited. Content may change prior to final publication. Citation information: DOI 10.1109/TSTE.2018.2878924, IEEE Transactions on Sustainable Energy

$$\frac{\partial i_{pv}}{\partial T} = \frac{n_p k_I \frac{\lambda}{\lambda_r} - n_p \frac{\partial I_s}{\partial T}\left(e^{\frac{q(v_{pv}+i_{pv}R_s)}{pKn_sT}} - 1\right) + \frac{n_p I_s q(v_{pv}+i_{pv}R_s)}{pKn_sT^2}\left(e^{\frac{q(v_{pv}+i_{pv}R_s)}{pKn_sT}}\right)}{1 + \frac{n_p I_s q R_s}{pKn_sT}\left(e^{\frac{q(v_{pv}+i_{pv}R_s)}{pKn_sT}}\right) + \frac{R_s}{R_{sh}}} \tag{10}$$

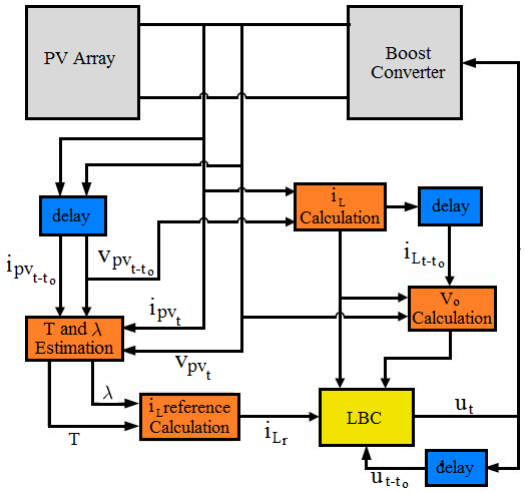

Fig. 4. Implementation of proposed control scheme along with MPPT

time history of available PV voltage and current measurement. Therefore, the cost of two additional sensors can be saved.From (5), i_L is written as

$$i_{L_t} = i_{pv_t} - C_a \frac{v_{pv_t} - v_{pv_{t-t_o}}}{t_o} \tag{24}$$

where t_o represents the time interval at which control action is updated. The variables i_{pv_t}, v_{pv_t}, $i_{pv_{t-t_o}}$ and $v_{pv_{t-t_o}}$ are the sensed PV currents and voltages at times t and $t - t_o$ respectively. Similarly, from (4), v_{o_t} is written as

$$v_{o_t} = \frac{v_{pv_t} - (1-u_t)V_D - r i_{L_t} - \frac{L}{t_o}\left(i_{L_t} - i_{L_{t-t_o}}\right)}{1-u_t} \tag{25}$$

Using above equations, the control action in (22) is updated using time history of i_{pv} and v_{pv} as given in (26) on the top of next page. Equation (26) shows that controller can be updated by sensing i_{pv} and v_{pv} only and does not need extra sensor on the output side. Block diagram in Fig. 4 shows various steps involved in the proposed MPPT algorithm.

VI. Results and Discussion

The proposed control scheme was implemented in MATLAB/Simulink and and was validated on experimental prototype. These details will be discussed in the following subsections.

TABLE II
PARAMETERS USED FOR SIMULATION AND HARDWARE IMPLEMENTATION

PV array parameter		Circuit parameter	
T_r	298K	C_a	$200\mu F$
λ_r	$1000W/m^2$	C_b	$200\mu F$
p	1	L	5mH
I_r	$1.37\text{x}10^{-8}$A	r	0.2Ω
I_{sc}	4.8A	V_d	0.6V
R_s	0.2Ω	Controller parameter	
R_{sh}	150Ω	f_s	20KHz
n_s	36	K_c	1.5
n_p	1	t_o	0.025s
		∂t	0.05s

A. Simulation Results

The performance of the proposed algorithm is simulated using MATLAB 2016a software on Intel core i3, 2.4GHz processor, 4GB RAM and Windows 7 operating system. PV array block has been used to simulate solar array. The operating temperature and irradiance can be given as external input and varied as desired. The parameters of the PV array block is shown in Table II. The pattern of variation in temperature and irradiance is shown in Fig. 5. The reference PV voltage and current values are given in Table I for these four cases. The estimated value of temperature and irradiance are obtained in Fig. 6 and Fig. 7 respectively using the procedure discussed in Section IV. It can be observed that the variation of estimated values are within 0.5% of their actual values. These values are estimated at the interval of $0.05s$. It is also observed that the two parameters reach their steady state value within $0.25s$. Although temperature is changed at $t = 2s$, there are some transients in estimated temperature at $t = 1s$ and $t = 3s$. Similarly transients are observed in irradiance estimation at $t = 2s$ when it is changed at $t = 1s$ and $t = 3s$. These transients are due to the fact that the calculation of one parameter is not independent from another. The P-V curve is changed if any of these two parameters is changed. These parameters cannot be correctly calculated if the two sets of voltage and currents are from different P-V curves. Once the P-V characteristic settles on a single curves, the parameter estimation is correctly done.

Figures 8 and 9 show the dynamics of desired, estimated and actual values of PV voltage and PV power respectively. Temperature and irradiance of PV array block are changed as per Fig. 5. Time taken to reach steady state values is $0.05s$. The desired, calculated and actual inductor current is shown in Fig. 10. It is to be noted that calculated inductor current tracks the actual current. The steady state ripple in calculated

This article has been accepted for publication in a future issue of this journal, but has not been fully edited. Content may change prior to final publication. Citation information: DOI 10.1109/TSTE.2018.2878924, IEEE Transactions on Sustainable Energy

$$u_{t+t_o} = \frac{(1-u_t)\left(v_{pv_t} - K_c L i_{L_r} + [K_c L - r]\left[i_{pv_t} - \frac{C_a}{t_o}\left(v_{pv_t} - v_{pv_{t-t_o}}\right)\right]\right)}{v_{pv_t} - r i_{L_t} - \frac{L}{t_o}\left((i_{pv_t} - i_{pv_{t-t_o}}) - \frac{C_a}{t_o}(v_{pv_t} - 2v_{pv_{t-t_o}} + v_{pv_{t-2t_o}})\right)} \tag{26}$$

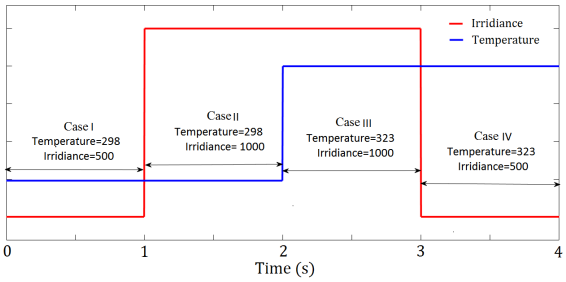

Fig. 5. Different cases of variation in temperature and irradiance

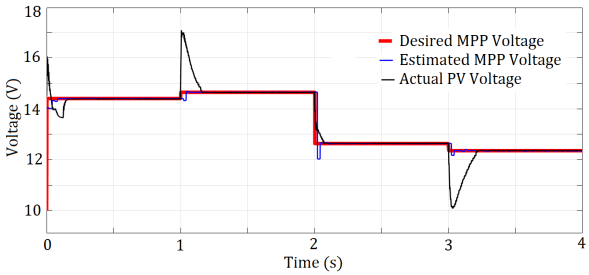

Fig. 8. Desired voltage, estimated voltage and actual current for MPP under different environmental conditions.

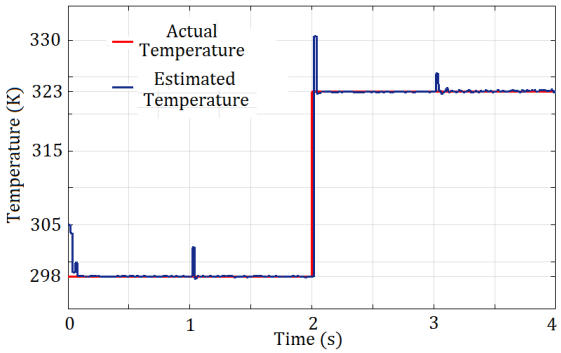

Fig. 6. Comparison of estimated temperature with actual value

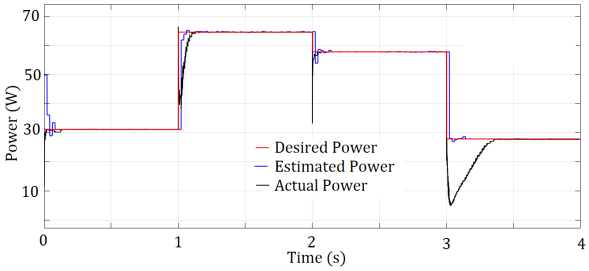

Fig. 9. Desired Power, estimated power and actual power for MPP under different environmental conditions.

inductor current is much lower compared to its actual value because the calculated inductor current is function of PV voltage and PV current which are constant in steady state. However, these transients are present in calculated inductor current whenever there is variation in operating conditions. The transient time depends on the input capacitor value. Fig.11 shows the variation in PV voltage, power and duty ratio when load is changed.

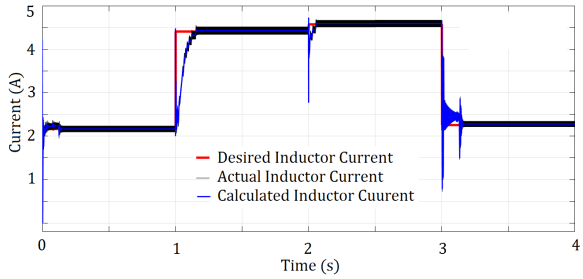

Fig. 10. Deisred, calculated and actual inductor current at MPP for different environmental conditions

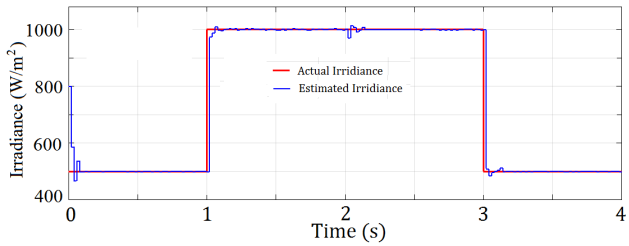

Fig. 7. Comparison of estimated irradiance with actual value

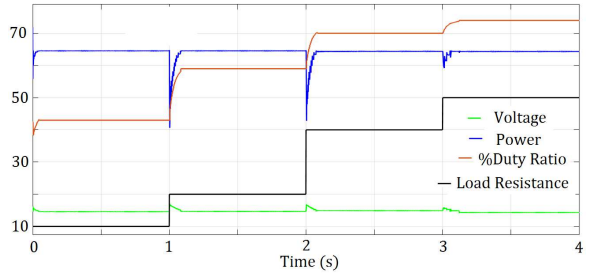

Fig. 11. PV voltage, power and duty ratio for different load conditions

This article has been accepted for publication in a future issue of this journal, but has not been fully edited. Content may change prior to final publication. Citation information: DOI 10.1109/TSTE.2018.2878924, IEEE Transactions on Sustainable Energy

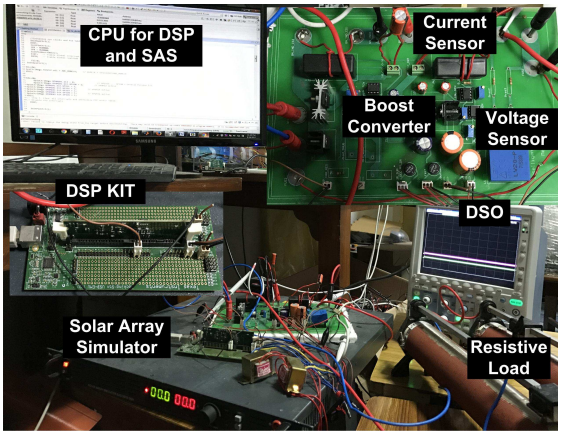

Fig. 12. Experimental setup for hardware implementation.

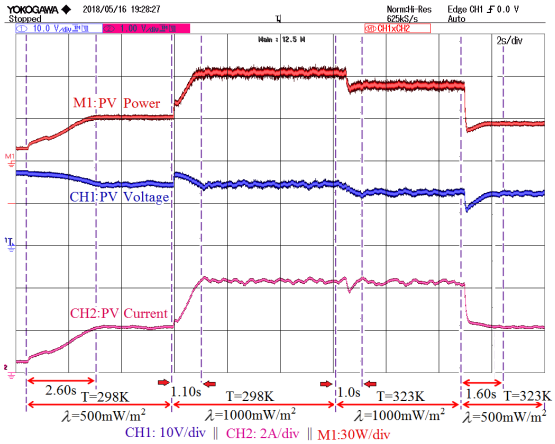

Fig. 13. Experimental waveform of PV power, PV voltage and PV current under varying temperature and irradiance at R_{ld}=30Ω using VSINC.

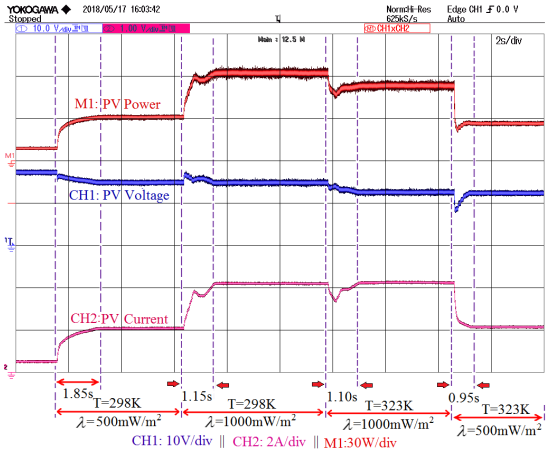

Fig. 14. Experimental waveform of PV power, PV voltage and PV current under varying temperature and irradiance at R_{ld}=30Ω using FC-MPPT.

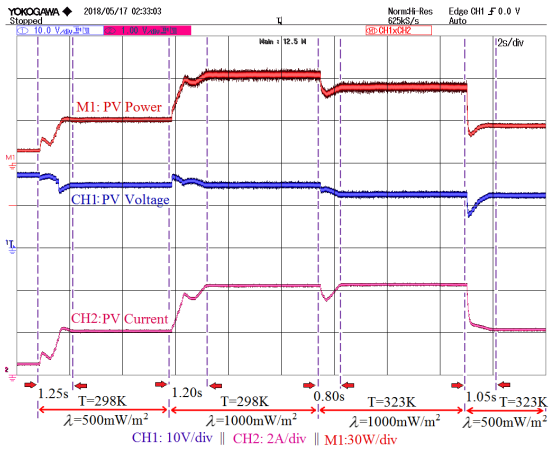

Fig. 15. Experimental waveform of PV power, PV voltage and PV current under varying temperature and irradiance at R_{ld}=30Ω using CMH-MPPT.

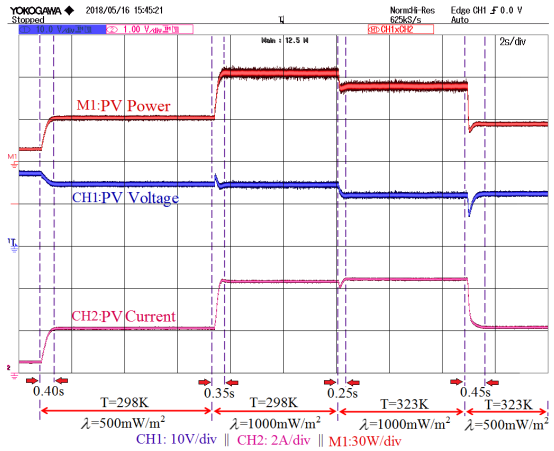

Fig. 16. Experimental waveform of PV power, PV voltage and PV current under varying temperature and irradiance at R_{ld}=30Ω using Proposed method.

B. Hardware implementation

The laboratory setup for the hardware implementation of the proposed scheme is shown in Fig.12. A solar array simulator manufactured by APLAB(SAS120/10) was used as a PV source. The P-V and I-V characteristics of the solar cell for different temperature and irradiation values were fed into the solar simulator using 50 points for each condition depicted in Fig 5. Thus, the SAS gives voltage and currents for the same parameters that are used in simulations. Hall effect Voltage sensor (LEM LV-20P) and current sensor (TELCON HTP 50) are used for sensing PV voltage and current respectively. Output of sensors are given to DSP kit (TMS320F28335) from Texas instrument which is used to implement the proposed MPPT algorithm.

The experiments are performed under two conditions (i) variation in environmental conditions (T & λ) (ii) variation in load. The results of proposed MPPT algorithm are compared with the results obtained from VSINC, FC-MPPT and CMH-MPPT methods. Fig. 13-16 show waveforms of voltage, current and power during MPPT using VSINC, FC-MPPT, CMH-MPPT and proposed MPPT method respectively at

This article has been accepted for publication in a future issue of this journal, but has not been fully edited. Content may change prior to final publication. Citation information: DOI 10.1109/TSTE.2018.2878924, IEEE Transactions on Sustainable Energy

a constant load of 30Ω. The controller was updated every $25ms$ for all the cases. The first transient in Fig. 13-16 shows initial MPPT process when the control action was first applied. The second, third and fourth transients depict the performance of various MPPT methods for irradiance increase (500 to $1000W/m^2$ at $298K$), temperature increase ($298K$ to $323K$ at $1000W/m^2$) and irradiance decrease (1000 to $500W/m^2$ at $323K$) respectively. From these results, it can be observed that when a transient occurs due to environmental change, initially, both the voltage and current rise/dip in the same direction. As the control action begins to take effect, the voltage and current values start to move in opposite directions. This observation confirms that the operating point has started to traverse the new P-V curve obtained after environmental change. MPPT process starts as soon as environmental change occurs for all MPPT methods but, is accomplished much faster for the proposed method. The reason for this is that the proposed method finds MPP point in a single step and estimates the duty ratio while other methods spend much time searching for MPP. Fig. 13-16 and Table-III show the performance of VSINC, FC-MPPT, CMH-MPPT and the proposed method. In all cases, the proposed MPPT converges very quickly and takes almost 66% less time. The average tracking time for VSINC, FC-MPPT and CMH-MPPT is 1.56s, 1.21s and 1.07s respectively while it is just 0.40s for the proposed method.

Fig. 17 (a)-(d) show the MPPT process for VSINC, FC-MPPT, CMH-MPPT and proposed MPPT method for varying load conditions. For this purpose, step change in resistive load was applied to the PV system at T=298K and λ=1000W/m^2. Initially system was run at MPPT for R=40Ω followed by two step changes from 40Ω to 20Ω and again 20Ω to 40Ω. The first transient in these waveforms shows MPP tracking when load resistance was changed from 40Ω to 20Ω. This transient shows instant drop in PV voltage due to increase in load causing deviation from MPP on the same I-V curve. Consequently, control action is applied and MPP voltage and maximum power is restored . Similarly the second transient shows instant rise in PV voltage due to decrease in load causing deviation from MPP. While the MPP voltage and maximum power remains same, the load voltage changes with variation in load. This is obvious because power is constant and resistance is different validating $P = V^2/R$ in steady state. It is clear from these waveforms that the proposed method is much faster than other three methods even for varying load conditions. The time taken by different MPPT techniques is tabulated in Table-III. Although the experiment was performed for changing resistive load, the proposed method is applicable to all kind of loads as it does not need any term involving load in its control law. Any change in load gets naturally reflected in PV voltage and PV current and appropriate control action gets applied.

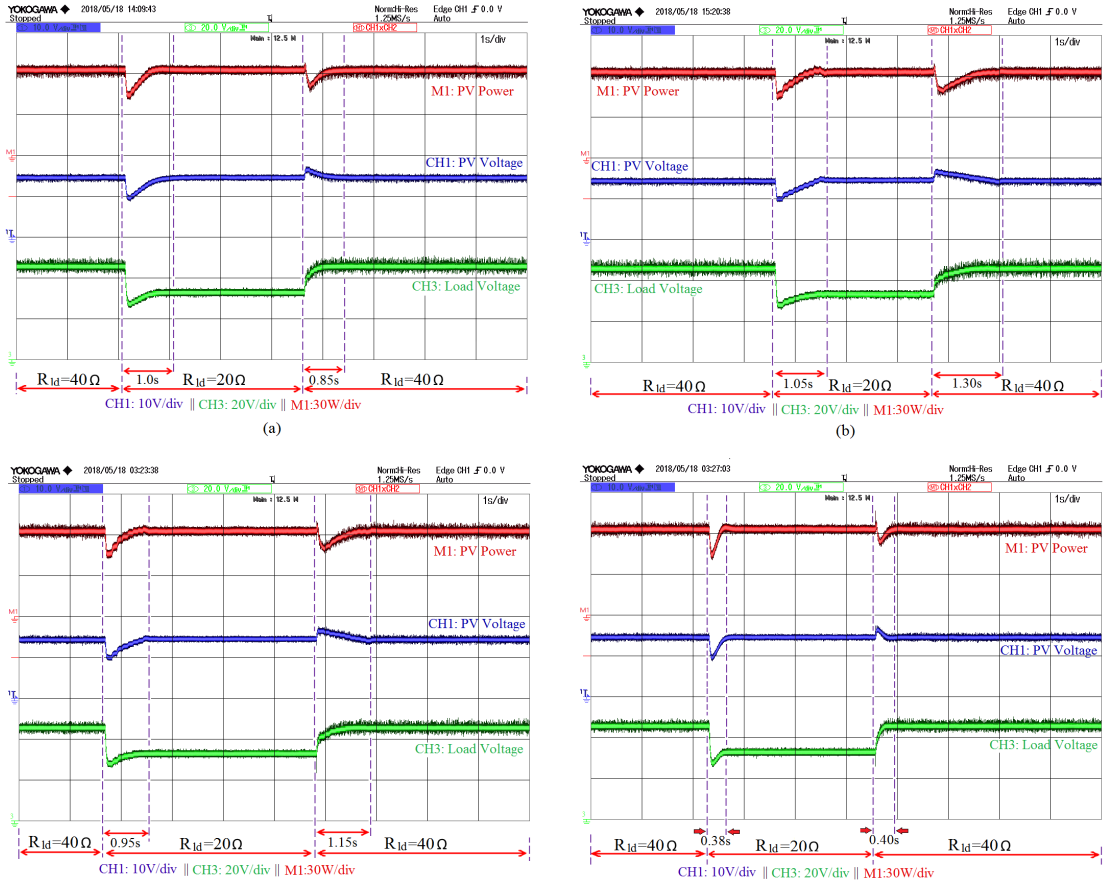

Fig. 17. Experimental waveforms of PV power, PV voltage and load voltage under varying load resistance at T=298 K and λ= 1000 W/m^2 using (a) VSINC (b) FC-MPPT (c) CMH-MPPT (d) proposed MPPT.

This article has been accepted for publication in a future issue of this journal, but has not been fully edited. Content may change prior to final publication. Citation information: DOI 10.1109/TSTE.2018.2878924, IEEE Transactions on Sustainable Energy

TABLE III
PERFORMANCE COMPARISON OF VARIOUS MPPT TECHNIQUES UNDER ENVIRONMENTAL AND LOAD VARIATIONS

Method	$\lambda = 500W/m^2$ to $\lambda = 1000W/m^2$	T=298K to T=323K	$\lambda = 1000W/m^2$ to $\lambda = 500W/m^2$	R_{ld}=40Ω to R_{ld}=20Ω	R_{ld}=20Ω to R_{ld}=40Ω
VSINC	1.1s	1.0s	1.6s	1.0s	0.85s
FC-MPPT	1.15s	1.1s	0.95s	1.05s	1.3s
CMH-MPPT	1.2s	0.8s	1.05s	0.95s	1.15s
Proposed Method	0.35s	0.25s	0.45s	0.38s	0.4s

VII. CONCLUSION

This paper presents a fast MPPT technique for photovoltaic array by estimating environmental conditions and load. For temperature and irradiance estimation, Newton-Raphson method has been applied to I-V characteristic of the PV array. Load was estimated by calculating inductor current and load voltage using boost converter dynamics. A Lyapunov based control law is derived to find optimum duty cycle according to different environmental conditions and load. Simulation and experimental results show that the proposed method is able to operate the PV array at MPP under varying environmental and load conditions. Performance of the proposed method was compared experimentally with three other MPPT methods present in literature. It is observed that the proposed method tracks MPP much faster than the other methods without any oscillation. The experimentally observed average MPP tracking times of proposed method for changing environment and load conditions are $0.40s$ and $0.39s$ respectively which are much smaller than the other three MPPT methods. Moreover, the proposed MPPT method is applicable to any kind of load as it is able to estimate the load using only PV voltage and PV current. In contrast to other techniques, the proposed method is able to find the value of duty cycle in single step for MPPT which otherwise is gradually found. This enables the proposed method to be free from multiple transients during MPPT and steady state oscillation. Furthermore, numerical calculation of inductor current and load voltage can be applied to other MPPT techniques to minimize number of sensors. Application of proposed method to the case of partial shading will be carried out in the future.

ACKNOWLEDGMENT

This research work is supported by the grants received from the Indian government bodies under the project SPO/DEITY/EE/2014090 and SERB/PDF/2016/001052.

REFERENCES

[1] S. Strache, R. Wunderlich, and S. Heinen, "A Comprehensive, Quantitative Comparison of Inverter Architectures for Various PV Systems, PV Cells, and Irradiance Profiles", *IEEE Trans. Sustain. Energy,* vol. 5, no. 3, pp. 813-822, Jul. 2014.

[2] A. K. S. Bhat and S. B. Dewan , " A novel utility interfaced high-frequency link photovoltaic power conditioning system ", *IEEE Trans. Ind. Electron. ,* vol. 35, no. 1, pp. 153-159, 1988.

[3] S. M. Alghuwainem, " Speed control of a PV powered DC motor driving a self-excited 3-phase induction generator for maximum utilization efficiency, ", *IEEE Trans. Energy Convers. ,* vol. 11, no. 4, pp. 768-773, 1996.

[4] E. Romero-Cadaval, G. Spagnuolo, L. G. Franquelo, C. A. Ramos-Paja, T. Suntio, and W. M. Xiao " Grid-Connected Photovoltaic Generation Plants: Components and Operation ", *IEEE Ind. Electron. Mag. ,* vol. 7, no. 3, pp. 6-20, Sep. 2013.

[5] J. D. Bastidas-Rodriguez, E. Franco, G. Petrone, C. A. Ramos-Paja, and G. Spagnuolo , " Maximum power point tracking architectures for photovoltaic systems in mismatching conditions: a review ", *IET Power Electron. ,* vol. 7, no. 6, pp. 1396-1413, 2014.

[6] A. Pallavee Bhatnagar and B. R. K. Nema , " Conventional and global maximum power point tracking techniques in photovoltaic applications: A review ", *J. Renew. Sustain. Energy ,* vol. 5, no. 3, p. 32701, May 2013.

[7] B. Subudhi and R. Pradhan , " A Comparative Study on Maximum Power Point Tracking Techniques for Photovoltaic Power Systems ", *IEEE Trans. Sustain. Energy ,* vol. 4, no. 1, pp. 89-98, Jan. 2013.

[8] N. Femia, D. Granozio, G. Petrone, G. Spagnuolo, and M. Vitelli , " Predictive & Adaptive MPPT Perturb and Observe Method ", *IEEE Trans. Aerosp. Electron. Syst. ,* vol. 43, no. 3, pp. 934-950, Jul. 2007.

[9] N. Femia, G. Petrone, G. Spagnuolo, and M. Vitelli , " Optimization of Perturb and Observe Maximum Power Point Tracking Method ", *IEEE Trans. Power Electron. ,* vol. 20, no. 4, pp. 963-973, Jul. 2005.

[10] M. A. Elgendy, B. Zahawi, and D. J. Atkinson , " Assessment of the Incremental Conductance Maximum Power Point Tracking Algorithm ", *IEEE Trans. Sustain. Energy ,* vol. 4, no. 1, pp. 108-117, Jan. 2013.

[11] B. W. Williams, A. A. Helal, M. A. Elsaharty, A. K. Abdelsalam, and N. E. Zakzouk , " Improved performance low-cost incremental conductance PV MPPT technique ", *IET Renew. Power Gener. ,* vol. 10, no. 4, pp. 561-574, Apr. 2016.

[12] M. Adly, H. El-Sherif, and M. Ibrahim , " Maximum power point tracker for a PV cell using a fuzzy agent adapted by the fractional open circuit voltage technique ", *2011 IEEE International Conference on Fuzzy Systems (FUZZ-IEEE 2011), 2011 ,* pp. 1918-1922.

[13] A. Sandali, T. Oukhoya, and A. Cheriti , " Modeling and design of PV grid connected system using a modified fractional short-circuit current MPPT ", *in 2014 International Renewable and Sustainable Energy Conference (IRSEC) ,* 2014, pp. 224-229.

[14] T. Esram, J. W. Kimball, P. T. Krein, P. L. Chapman, and P. Midya , " Dynamic maximum power point tracking of photovoltaic arrays using ripple correlation control ", *IEEE Trans. Power Electron. ,* vol. 21, no. 5, pp. 1282-1291, Sep. 2006.

[15] M. Rakhshan, N. Vafamand, M. H. Khooban, and F. blaabjerg , " Maximum Power Point Tracking Control of Photovoltaic Systems: A Polynomial Fuzzy Model-Based Approach ", *IEEE J. Emerg. Sel. Top. Power Electron. ,* pp. 1-1, 2017.

[16] N. A. Rahim, A. Che Soh, M. A. M. Radzi, and M. A. A. M. Zainuri , " Development of adaptive perturb and observe-fuzzy control maximum power point tracking for photovoltaic boost dcdc converter ", *IET Renew. Power Gener. ,* vol. 8, no. 2, pp. 183194, Mar. 2014.

[17] K. L. Lian, J. H. Jhang, and I. S. Tian , " A Maximum Power Point Tracking Method Based on Perturb-and-Observe Combined With Particle Swarm Optimization ", *IEEE J. Photovoltaics ,* vol. 4, no. 2, pp. 626633, Mar. 2014.

[18] K. Ishaque, Z. Salam, M. Amjad, and S. Mekhilef , " An Improved Particle Swarm Optimization (PSO)Based MPPT for PV With Reduced Steady-State Oscillation ", *IEEE Trans. Power Electron. ,* vol. 27, no. 8, pp. 36273638, Aug. 2012.

[19] L. M. Elobaid, A. K. Abdelsalam, and E. E. Zakzouk , " Artificial neural network-based photovoltaic maximum power point tracking techniques: a survey ", *IET Renew. Power Gener. ,* vol. 9, no. 8, pp. 10431063, Nov. 2015.

[20] Y. Shaiek, M. B. Smida, A. Sakly, and M. F. Mimouni , " Comparison between conventional methods and GA approach for maximum power point tracking of shaded solar PV generators ", *Sol. Energy ,* vol. 90, pp. 107-122, Apr. 2013.

[21] M. Khaled, H. Ali, M. Abd-El Sattar, and A. A. Elbaset , " Implementation of a modified perturb and observe maximum power point tracking algorithm for photovoltaic system using an embedded microcontroller ", *IET Renew. Power Gener. ,* vol. 10, no. 4, pp. 551-560, Apr. 2016.

[22] F. Liu, S. Duan, F. Liu, B. Liu and Y. Kang, "A Variable Step Size INC MPPT Method for PV Systems," *IEEE Transactions on Industrial Electronics,* vol. 55, no. 7, pp. 2622-2628, July 2008.
[23] T. K. Soon and S. Mekhilef, "A Fast-Converging MPPT Technique for Photovoltaic System Under Fast-Varying Solar Irradiation and Load Resistance," *IEEE Transactions on Industrial Informatics,* vol. 11, no. 1, pp. 176-186, Feb. 2015.
[24] L. M. Elobaid, A. K. Abdelsalam and E. E. Zakzouk, "Artificial neural network-based photovoltaic maximum power point tracking techniques: a survey," *IET Renewable Power Generation,* vol. 9, no. 8, pp. 1043-1063, 11 2015.
[25] H. Abu-Rub, A. Iqbal, S. Moin Ahmed, F. Z. Peng, Y. Li and G. Baoming, "Quasi-Z-Source Inverter-Based Photovoltaic Generation System With Maximum Power Tracking Control Using ANFIS," *IEEE Transactions on Sustainable Energy,* vol. 4, no. 1, pp. 11-20, Jan. 2013.
[26] M. G. Villalva J. R. Gazoli E. R. Filho "Comprehensive approach to modeling and simulating photovoltaic arrays" *IEEE Trans. Power Electron.* vol. 24 no. 5 pp. 1198-1208 May 2009.
[27] H. S. Sahu and S. K. Nayak, "Estimation of maximum power point of a double diode model photovoltaic module," *IET Power Electronics,* vol. 10, no. 6, pp. 667-675, 5 19 2017.
[28] M. Haouari-Merbah, M. Belhamel, I. Tobas, J.M. Ruiz, "'Extraction and analysis of solar cell parameters from the illuminated current-voltage curve", *Solar Energy Materials and Solar Cells,* Volume 87, Issues 14, 2005.
[29] Jen-Cheng Wang, Yu-Li Su, Jyh-Cherng Shieh, Joe-Air Jiang, High-accuracy maximum power point estimation for photovoltaic arrays, *Solar Energy Materials and Solar Cells,* Volume 95, Issue 3,2011
[30] J. J. Soon and K. S. Low, "Photovoltaic Model Identification Using Particle Swarm Optimization With Inverse Barrier Constraint," *IEEE Transactions on Power Electronics,* vol. 27, no. 9, pp. 3975-3983, Sept. 2012.
[31] E. I. Batzelis, G. E. Kampitsis, S. A. Papathanassiou, and S. N. Manias , " Direct MPP Calculation in Terms of the Single-Diode PV Model Parameters ", *IEEE Trans. Energy Convers. ,* vol. 30, no. 1, pp. 226-236, Mar. 2015.
[32] Y. Mahmoud, M. Abdelwahed and E. F. El-Saadany, "An Enhanced MPPT Method Combining Model-Based and Heuristic Techniques," *IEEE Transactions on Sustainable Energy,* vol. 7, no. 2, pp. 576-585, April 2016.
[33] M. Jedari Zare Zadeh and S. H. Fathi, "A New Approach for Photovoltaic Arrays Modeling and Maximum Power Point Estimation in Real Operating Conditions," *IEEE Transactions on Industrial Electronics*, vol. 64, no. 12, pp. 9334-9343, Dec. 2017.
[34] N. Femia, G. Petrone, G. Spagnuolo, and M. Vitelli, *Power Electronics and Control Techniques for Maximum Power Harvesting in Photovoltaic Systems* . Boca Raton, FL, USA: CRC Press, 2013.
[35] Ahmed. A, Li. R, Moon. S, Park. J. H , " A Fast PV Power Tracking Control Algorithm With Reduced Power Mode ", *EEE JOURNAL OF PHOTOVOLTAICS. ,* vol. 28, no. 3, pp. 565-575, Sep. 2013.
[36] Jadli. U, Thakur. P, Shukla. R, " A New Parameter Estimation Method of Solar Photovoltaic ", *IEEE Trans. Energy Convers. ,* vol. 8, no. 1, pp. 239-247, Jan. 2018.
[37] Soto. W, Klein. S.A, Beckam. W.A, " Improvement and validation of a model for photovoltaic array performance ", *ELSEVIER. SOLAR ENERGY ,* vol. 80, no. 1, pp. 78-88, Jan. 2006.
[38] R. Haroun, A. E. Aroudi, A. Cid-Pastor, G. Garcia, C. Olalla and L. Martnez-Salamero, "Impedance Matching in Photovoltaic Systems Using Cascaded Boost Converters and Sliding-Mode Control," *IEEE Transactions on Power Electronics,* vol. 30, no. 6, pp. 3185-3199, June 2015.
[39] A. Hussain, A. Kumar, and L. Behera , " Sliding mode control of a buck converter for maximum power point tracking of a solar panel ", *2013 IEEE International Conference on Control Applications (CCA), 2013 ,* pp. 661-666.
[40] S.S. Ge. *LYAPUNOV DESIGN* [Online]. Available: https://robotics.nus.edu.sg/sge/journal/bookchapter/bookchapter LyapunovDesign.pdf.

Amir Hussain received his B.Tech degree in Electrical Engineering from MNNIT Allahabad in 2010 and M.Tech degree in Power and Control from IIT Kanpur in 2013. He worked as Project Engineer in Intelligent System and Control Laboratory, IIT Kanpur from Feb 2017 to Jul 2018. He is currently pursuing PhD in electrical engineering at University of Houston. His area of research include control of power electronics converter, grid connected inverter and renewable energy conversion.

Man Mohan Garg received his B.E. (Electrical Engineering) from the M.B.M. Engineering College Jodhpur, India, in 2008 and M.Tech and Ph.D from Department of Electrical Engineering, Indian Institute of Technology (IIT) Roorkee, India in 2010 and 2016, respectively. He has completed his Post-doctoral research work (under the prestigious N-PDF scheme sponsored by SERB, India) in the Department of Electrical Engineering, Indian Institute of Technology (IIT) Kanpur, India. He is currently working as Assistant Professor at Department of Electrical Engineering, National Institute of Technology (NIT) Rourkela, India. His current research interests include design, modeling and control of power electronic converters, grid integration of distributed renewable energy sources, dc microgrid, cyber-physical energy systems etc. He has published research papers in IEEE Transactions on Power Electronics, other reputed international journals and conferences. He is an active reviewer for several IEEE Transactions, reputed journals and conferences.

Meher Preetam Korukonda received the B.Tech degree in Electrical Engineering from National Institute of Technology Durgapur, Durgapur, West Bengal, India in 2011. He is currently a doctoral student at the Department of Electrical Engineering, Indian Institute of Technology Kanpur, Kanpur, Uttar Pradesh, India. He previously worked as a Project Associate at Intelligent Systems and Control Laboratory, IIT Kanpur, India. His research interests include cyber-physical systems, intelligent control and smart grid.

Shamim Hasan received the B.Tech. degree in Electrical Engineering from Maharana Pratap Engineering College, Kanpur, India, in 2010, and the M.Tech. degree, in Electrical Engineering from Indian Institute of Technology Kanpur, India, in 2013. He is currently working toward the PhD degree in Department of Electrical Engineering at Indian Institute of Technology Bombay, India.

From January 2014 to December 2015, he worked as a member of the faculty in Department of Electrical and Electronics Engineering, PSIT, Kanpur, India. He also worked as a Project Engineer at Intelligent Systems and Control Laboratory, IIT Kanpur, India. His research interests include control of grid connected converters, microgrid and power quality improvement.

This article has been accepted for publication in a future issue of this journal, but has not been fully edited. Content may change prior to final publication. Citation information: DOI 10.1109/TSTE.2018.2878924, IEEE Transactions on Sustainable Energy

Laxmidhar Behera received the BSc (engineering) and MSc (engineering) degrees from NIT Rourkela in 1988 and 1990, respectively. He received the PhD degree from IIT Delhi in 1996. He is currently working as the professor in the Department of Electrical Engineering, IIT Kanpur. He is also a guest professor in Hangzhou Dinazi University, China. He has worked as an assistant professor at BITS Pilani during 1995-1999 and pursued the postdoctoral studies in the German National Research Center for Information Technology, GMD, Sank Augustin, Germany, during 2000-2001. He worked as the reader in Intelligent Systems Research Center (ISRC), University of Ulster, United Kingdom during 2008-2010. He has also worked as a visiting researcher/professor at FHG, Germany, and ETH, Zurich, Switzerland. He has more than 200 papers to his credit published in refereed journals and conference proceedings. His research interests include intelligent control, robotics, semantic signal/ music processing, neural networks, control of cyber-physical systems and cognitive modeling. He is Fellow of Indian National Academy of Engineering.